Available online at www.sciencedirect.com
ScienceDirect
Food Hydrocolloids 21 (2007) 986–995
FOOD HYDROCOLLOIDS
www.elsevier.com/locate/foodhyd

In-vivo visualisation of mouth–material interactions by video rate endoscopy

Sarah Adams[a,*], Scott Singleton[b], Rimas Juskaitis[c], Tony Wilson[c]

[a]*Physical and Engineering Sciences, Unilever Corporate Research, Colworth Park, Bedford MK44 1LQ, UK*
[b]*Measurement Science, Unilever Research, Colworth Park, Bedford MK44 1LQ, UK*
[c]*Department of Engineering Science, University of Oxford, Parks Road, Oxford OX1 3PJ, UK*

Received 18 April 2006; accepted 14 August 2006

Abstract

Results are reported for the first time on the use of an in-vivo fluorescence imaging technique to visualise residue in the oral cavity after oral processing of model fluid foods. A rigid rod endoscope is mounted such that all major axes of motion (pitch, yaw, roll, forward/reverse) can be exploited allowing comfortable viewing conditions for the subject during extended viewing periods. The technique has been applied to investigate the in-mouth behaviour, the distribution and clearance, of a range of homogeneous fluid foods in a subject. The results indicate that, for a range of different CMC solutions of varying citric acid content, viscosity is a key indicator for initial residue amount whereas salivary flow rate was shown to have little or no effect on initial deposited amount. However, salivary flow rate was found to have a strong influence on how quickly material was cleared from the oral cavity, with higher rates leading to faster clearance. The technique was also used to follow the in-mouth behaviour of bulk samples of corn and castor oil. Rapid emulsification on oral processing was observed, with smaller average droplet size observed for the lower viscosity oil. This work demonstrates the potential of this technique for investigating the range of processes that occur in the mouth during food processing and opens up new possibilities to increase our understanding of food material behaviour and its potential impact on the sensory perception of foods.

Keywords: In-vivo imaging; Fluorescence endoscopy; Food residue; Clearance

1. Introduction

The bulk physical properties and 3-D microstructure of a food material has a crucial effect on its sensory perception. There has been significant effort directed towards understanding the links between the bulk material properties of foods and their sensory properties (Bourne, 2002; Moskowitz, 1987) and there is a long history of process control during manufacture to optimise product properties for sensory preference. Most work has focussed on controlling the microstructure of the final product before it reaches the consumer whereas it is likely that the way in which the product interacts with the 3-D structures of the oral cavity during eating is what ultimately determines the physiological stimuli the food induces and the resulting sensory perception. Hence, recent work has been conducted to try to probe how the properties of the food material change upon oral processing whilst the product is in use and ultimately what the impact of these changes and interactions may be on sensory perception (De Wijk, Engelen, & Prinz, 2003; Engelen et al., 2003; Engelen, de Wijk, Prinz, van der Bilt, & Bosman, 2003; Lucas, Prinz, Agrawal, & Bruce, 2002; Peleg, 2006; Vingerhoeds, Blijdenstein, Zoet, & van Aken, 2005).

Here, we report for the first time the in-vivo visualisation of food materials inside the oral cavity using a video rate endoscopy device. This device allows us to collect sub millimetre resolution, real-time images of the mucosal surfaces from around the oral cavity of a subject in a natural sitting position both before and after consumption of food. The images reveal information on the structures within the oral cavity and on the product residue after eating. This allows us to directly probe food material

*Corresponding author. Tel.: +44 1234 222554; fax: +44 1234 222152.
E-mail address: sarah.adams@unilever.com (S. Adams).

0268-005X/$ - see front matter © 2006 Elsevier Ltd. All rights reserved.
doi:10.1016/j.foodhyd.2006.08.011

breakdown and deposition onto oral surfaces, both key parameters in the sensory perception of foods.

The aim of this work is to introduce the in-vivo imaging technique and demonstrate its effectiveness in giving quantitative information about food residues after consumption. As well as presenting detailed images of the structures inside the oral cavity and their response to certain stimuli, we also present work investigating the in-mouth behaviour of a range of viscous fluids in a single subject. Carboxy methyl cellulose (CMC) is a relatively tasteless polysaccharide commonly used in the food industry as a stabiliser or thickening agent (E468). Here, we use a series of different concentration CMC solutions to generate fluids with viscosities in the range 0.01–10 Pa.s to investigate the influence of viscosity on product residue. We also present results from a study of CMC solution containing different levels of citric acid, a known salivary stimulant (Watanabe & Dawes, 1988) to investigate its influence on residue clearance. Finally, we present images collected from the oral cavity after consumption of viscous oils. This clearly shows the emulsification that takes place during consumption.

2. Materials and methods

2.1. Materials, sample preparation and characterisation

In order to minimise taste elements from the in-mouth behaviour, CMC solutions were prepared in a tasteless salt solution (TSS). The composition of the TSS was taken from the work of Kringelback, O'Doherty, Rolls, and Andrews (2003). TSS was prepared by dissolving different salts into bottled drinking water (Highland Spring still mineral water). NaCl, $NaHCO_3$ and KCl were added to give a final ionic composition similar to that of saliva (see Table 1). Riboflavin, a naturally fluorescent, highly water-soluble vitamin (B2) (Sigma) was added to the TSS to a final concentration of 0.03 mM as a fluorescent marker. The CMC used was supplied by Hercules, Wilmington DE (Blanose 7MF) and used as supplied. Solutions were prepared by adding the dry CMC to the TSS under stirring. The samples were then continuously stirred until all of the CMC had dissolved. The concentrations of CMC were chosen to give viscosities in the range 0.01–10 Pa.s at a shear rate of $10\,s^{-1}$. The steady shear viscosity of the samples was measured at 25 °C using a Rheometrics ARES rheometer with a cone and plate geometry. The viscosity data are shown in Fig. 1. The level of fluorescence from the samples was assessed using a Perkin Elmer LS50B spectro-fluorimeter and was found to be identical for all samples in the series to within experimental error.

In order to investigate the effect of tastant level a series of 0.1 Pa.s CMC solutions were prepared with 0.03 mM riboflavin and varying levels of citric acid (Jungbunzlauer), 0, 5, 12.5, 25 or 50 mM. The addition of citric acid was found to have no significant impact on the rheology or the fluorescence of the samples. Fluorescence levels between

Table 1
'Tasteless salt solution' composition

	Species	Concentration (mM)
Added salts	NaCl	2.0
	$NaHCO_3$	0.3
	KCl	23.0
Final ion content	Ca	0.9
	Mg	0.35
	Na	2.6
	K	23.0
	HCO_3	2.5
	Cl	0.06
	SO_4	Trace
	NO_3	Trace
	F	Trace
	Fe	Trace
	Al	Trace

The solution was prepared by dissolving salts into Highland Spring mineral water. The levels of added salt are listed together with the final expected ion concentration in the solution.

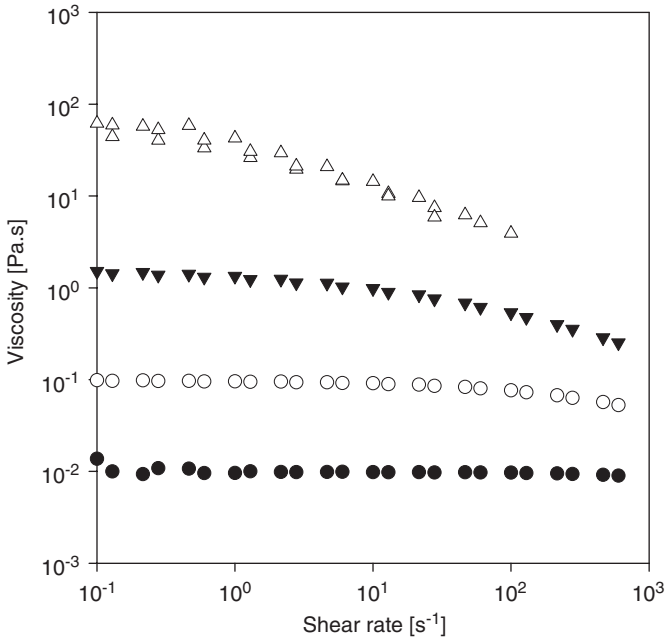

Fig. 1. Steady shear rheology of a solution of CMC in TSS with varying CMC concentration, ● 0.62 wt%, ○ 1.46 wt%, ▼ 2.83 wt% and ▽ 5.50 wt%.

the viscosity series and the acid series did differ slightly, due to experimental errors in the riboflavin concentration. Each series was therefore analysed separately.

Most food oils were found to have a similar Newtonian behaviour (data not shown) and corn oil (Tesco's own brand), with a viscosity of 0.05 Pa.s measured at 25 °C, was selected for its low odour and bland taste. Castor oil (pharmaceutical grade from J & W Whewell Ltd) was selected as it presents a significantly higher viscosity than other edible oils, 0.64 Pa.s measured at 25 °C. Circumin (Fluka) was added to the oils as a fluorescent label.

Circumin is a naturally fluorescent extract of the spice cumin and is highly soluble in food oils with negligible fluorescence in the aqueous phase of oil water and oil saliva mixtures. Further to this, experiments using freshly collected cheek cells demonstrate that, under conditions that simulate the swill and spit conditions of the in-mouth experiments, circumin does not interact with the phospholipids of these cells. However, the quantum yield for the fluorescence of circumin is very different in the different oils. The concentration of circumin added to the oils was therefore adjusted to attempt to account for this (0.08 wt% circumin in corn oil and 0.002 wt% circumin in castor oil). Fig. 2 shows the fluorescence spectra for the oil samples used in this study. This sensitivity of the quantum yield to environment limits the use of circumin for fully quantitative analysis in the potentially rapidly changing environment of the mouth.

An aqueous solution of sodium fluorescein (Sigma) was used as a fluorescent marker for the oral surfaces.

All samples were cleared for bacteriological safety before use in human subjects.

2.2. Video rate endoscopy apparatus

Previously, two of the authors have described the principles of video-rate confocal endoscopy as applied to accessible regions of the body, including the oral cavity (Watson, Neil, Juskaitis, Cook, & Wilson, 2002). This earlier work allowed verification of the low power dosage to the tissue and the absence of any heating or discomfort to the volunteers under illumination and imaging conditions. In addition, the laser power delivered to the endoscope was kept within the recommended radiance dosage guidelines (BS EN 60825-1, 1994) allowing safe, continuous repeat experimentation. Finally the endoscope is designed for clinical applications and is therefore simple to maintain hygienically.

In their earlier work, Watson et al. (2002) developed technology to deliver a range of functional applications. In particular, both fluorescent imaging/spectroscopy and reflectance imaging are possible and, since image contrast in both these configurations can be generated from surface and subsurface regions, they found it advantageous to introduce the capability for confocal imaging. Fluorescent labelling of the mouth structures was found to produce greater differentiation between the features of interest. Finally, highest quality signal to noise images with good temporal and spatial resolution required a 'fast' all digital approach to image acquisition. In this report, we further extend the principles described by Watson et al. (2002) to allow comfortable viewing conditions for the volunteer subject during extended viewing periods from within the oral cavity and optimise the system for fluorescence-based imaging of food materials in the oral cavity. The extended integrated configuration developed in this work is shown in Fig. 3 together with a representative view of the instrument in operation. (In this work no fluorescence spectroscopy (requiring a dispersive monochromator) has yet been incorporated and no confocal images were collected. However, the design is fully compatible with the 'drop-in' incorporation of these functions, as shown.)

The instrument design is completed by mounting around optical bench components (Tube Mounting System C, Linos, Germany) such that all the major axes of movement (pitch, yaw, roll, forward/reverse) can be accommodated and hence exploited by the volunteer (as shown in Fig. 3). In addition the optical design maintains fully enclosed on-axis illumination and imaging conditions for the endoscope

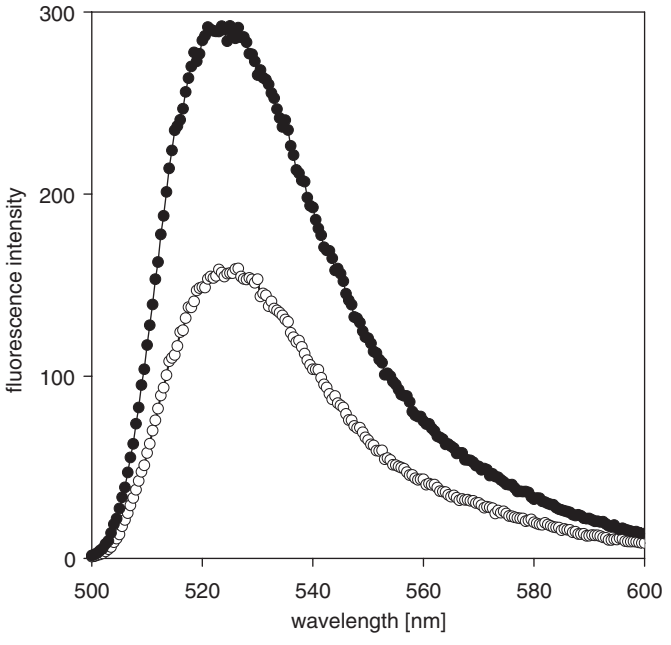

Fig. 2. Fluorescence emission spectra from circumin labelled oil samples excited at 488 nm, —●— 0.002 wt% circumin in castor oil and —○— 0.08 wt% circumin in corn oil.

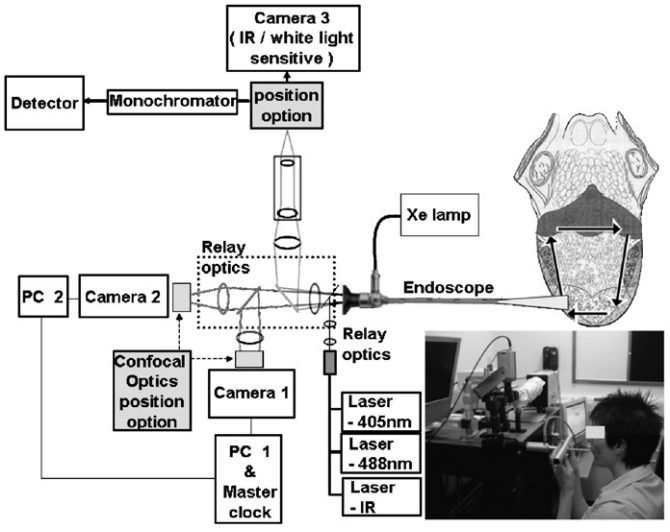

Fig. 3. Schematic representation of the in-vivo video rate confocal endoscopy apparatus. The insert shows the system in use.

throughout its movement range. This flexibility also allows for good contact to be maintained between the endoscope distal lens and the oral surface under investigation, mediated by the salivary film. This type of contact has been shown to be sufficient for reducing the potential for strong reflections (Watson et al., 2002).

2.2.1. Endoscope

In this work, a rigid endoscope (Hopkins type contact telescope: Karl Storz, Tuttlingen, Germany) was used, that was similar to the selection described in Watson et al., 2002. The endoscope has an external diameter of 4 mm, is ~20 cm in length and contains an internal focussing mechanism and a 30° forward angle lens for imaging structures lateral to the axis of the instrument as this was found to be particularly suitable for imaging the rear aspects of the tongue and cheek surfaces.

2.2.2. Illumination

Conventional (non-confocal) images could be obtained using the incoherent lamp source and liquid light guide supplied as part of the original endoscope package. This is introduced directly into the relay optics in the endoscope and therefore produces a non-confocal reflected light image. Hence, in this mode the image contrast, which is essentially dark-field in nature, is obtained from light backscattered from the sample. This image mode is particularly suitable to study the 'just' subsurface distribution and behaviour of capillary loops and blood flow through the tongue, cheek and lip structures.

The principle mode of illumination exploited a series of laser sources, moderated to deliver a maximum power of 4 mw, across ~2 mm^2 viewing field to the mouth surface. Laser sources were a frequency doubled Sapphire diode laser operating at 488 nm (Coherent, USA), a Chromalase diode laser at 405 nm (Blue Sky Research, USA) and a high brightness 810 nm LED (ELJ-810-228B, Epigap, Germany). The visible laser sources were required to provide the illumination for all fluorescence image sequences, whilst the IR laser provides a reference surface image that the volunteer uses when scanning the surface of the tongue.

Flexibility in design of the relay optics on the emission side of the instrument allows rapid exchange of dichroic and barrier filters. Hence, single channel fluorescence imaging could be achieved using barrier filters suitable for 405 nm excitation based emission or 488 nm excitation based emission by appropriate filter selection in the emission pathway. Alternatively, dual channel and simultaneous fluorescence emission imaging following dual 405 and 488 nm excitation is possible using combinations of dichroic (Omega Optical, USA 400-485DBDR, 450DCLP, 488DRLP and 675DCSPXP) and bandpass filters (Semrock, USA FF562-Ex02-A and FF409-Em02-B).

2.2.3. Camera and image grabbing

Dual 14 bit cooled EMCCD cameras (1004 × 1002 pixels) (Ixon-885, Andor Bioimaging, Nottingham, UK) were used throughout this work. These cameras provide sufficient sensitivity for real-time fluorescence imaging of weakly fluorescent food materials/structures in the mouth up to several minutes post consumption. Imaging conditions varied during this work—depending upon experimental regime however, typically 10 ms exposure times and 15–25 frames per second were gathered. The cameras could by synchronised to ensure simultaneous imaging of the same spatial zone in dual fluorescence mode.

Images were directly digitally captured, to maintain information content using supplied software (Andor Bioimaging Ltd). Simple image analysis procedures to correct for illumination gradients and background subtraction could be developed in this software and hence allow direct quantification of fluorescent signals.

2.3. Experiment protocol

In each case, the subject was a healthy volunteer and was instructed to prepare their mouth for the study by brushing the teeth and tongue prior to any images being collected. The subject then sat quietly to allow the mouth to return to a 'normal' state, as measured by self-reporting and ensuring that salivary flow rate had returned to a consistent resting level, before starting experiments. Images could then be collected from inside the oral cavity. Where fluorescent labelling of the oral structures was required, the area was treated locally with a drop of sodium fluorescein solution in water (0.05 wt%) prior to any images being collected.

In order to assess the in-mouth behaviour of the model fluid foods, the subject adhered to the following protocol. A series of images were collected from around a predetermined path on the surface of the tongue. Data was collected from the right-hand side of the tongue, the back, the left-hand side and the tip of the tongue in sequence (see Fig. 3) with approximately 100 frames collected from each region. The subject was in control of the endoscope at all times and probed as far back on the tongue as was comfortable (covering predominantly the anterior two thirds of the tongue). This constituted the background or resting state of the mouth. A resting salivary flow rate was also measured by collecting the subject's saliva in a pre-weighed vessel over a 1 min period. The subject was then asked to take a measured 5 ml aliquot of sample into their mouth and to swill for 30 s. After this time, the subject was told to expectorate the sample and more images were collected from the same predetermined path on the tongue. A stimulated salivary flow rate was then measured by collecting saliva for 1 min. Subsequent scans were collected at various time intervals after initial sample ingestion.

2.4. Data handling

In order to analyse the data collected from food residues for residue amount, the illumination profile of the images

had to be corrected across the whole field of view. This was achieved by ratioing the images with an image collected by immersing the endoscope tip directly into a homogeneous fluorescent solution. The corrected data were then analysed, frame-by-frame, for mean intensity. Subtraction of the mean intensity recorded from the autofluorescence of the mouth during the background image sequence then gives a value for the fluorescent intensity that is directly proportional to the amount of product residue assuming no or undifferentiated quenching processes.

3. Results and discussion

3.1. Imaging of oral structures

3.1.1. White light reflectance imaging

Using non-confocal epi-illumination allows for visualisation of the near-surface aspects and patterns of arterioles and capillary loops supplying blood in the mouth, see Fig. 4. Indeed, the flow of individual red blood corpuscles in individual capillary loops could be seen in real-time video sequences taken from a range of sites (cheek, tongue, etc.). This imaging mode was used to measure the response of the blood flow in the capillaries to the thermal stimulus of a block of ice applied to the inner surface of the cheek. Fig. 4b shows a clear reduction in the contrast of the capillaries as compared to the pre treatment image, Fig. 4a. This is related to the reduced blood flow in response to the cold stimuls.

3.1.2. Fluorescence imaging

Non-confocal fluorescence imaging was then undertaken from various sites within the mouth by applying an aqueous solution of sodium fluorescein to provide strong contrast for these images. Fig. 5 shows single frame fluorescent images taken from the real-time sequences collected. The use of a strong contrast agent provides highly detailed 'surface dominated' information within the mouth in a very simple form with good spatial and temporal resolution. The images show a level of cellular and morphological detail. Figs. 5a and b both show the structure of the tongue surface but from different aspects. Fig. 5a was recorded from near the middle of the tongue whereas Fig. 5b was recorded from the posterior surface. This clearly identifies the very different structures in these two areas, with very different length scales. These differences in structure could have a significant effect on how food materials interact with different regions of the tongue. In Fig. 5b, fluorescein has visibly pooled in the 'gutters' around the fungiform papillae. In both Fig. 5a and b, cellular level detail of the papillae can be discerned. Also shown in Fig. 5c is an image of one of the salivary ducts at the posterior of the mouth.

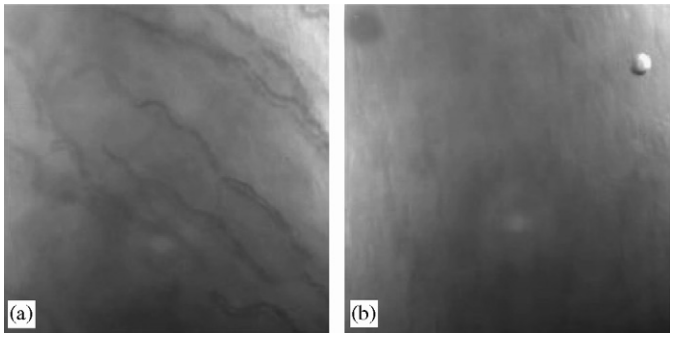

Fig. 4. Incoherent epi-illumination white light images from the inner surface of the cheek before (a) and after (b) application of a block of ice. The image width is ~1.5 mm. The capillary network is clearly visible just below the mucosal surface in image (a). The reduction in blood flow in response to the application of the ice is clearly identified by a lack of structure visible in image (b).

3.2. Imaging of model fluid food residues

Non-confocal fluorescent imaging was used to collect data on the food residues remaining on the surface of the tongue after oral processing of a range of model fluid foods.

3.2.1. Influence of viscosity in homogeneous aqueous fluids

Fig. 6 shows an image recorded from the right hand side of the tongue immediately after a riboflavin-labelled 1.46 wt% solution of CMC had been swilled and then expectorated. The pattern of coverage shown is typical for all of the aqueous samples studied. The inhomogeneous coverage can be related to the underlying structure of the tongue.

The images were analysed for mean intensity and the mean intensity recorded from the background scan of the mouth, before any samples were ingested, was subtracted. Fig. 7 shows a plot of the background corrected mean intensity vs. normalised circuit time (taken from the frame number of the video image). The subject scanned a 'square' on the tongue surface at constant rate, the circuit time could then be related to the position of the endoscope on the tongue. In total 400 frames were collected from around the square, these have been normalised such that on Fig. 7, the region between 0 and 0.25 relates to travelling from the tip to the back of the tongue along the right-hand edge of the tongue, 0.25–0.5 to crossing the back of the tongue from right to left, 0.5–0.75 to traversing the left-hand side of the tongue and 0.75–1 to the tip of the tongue. This plot gives information on the pattern of the residue distribution around the surface of the tongue. For example, it is clear from Fig. 7 that the subject had a preference for the right-hand side of their mouth. It is also evident that material was cleared much more quickly from the tip of the tongue, the signal intensity is essentially zero by the second time point. This is as would be expected as the tip of the tongue contacts the other surfaces of the mouth much more frequently and this would contribute to the cleaning effect.

Averaging the intensity data over all frames gives an indication of the total amount of food residue present at the time of data collection. Fig. 8 shows a plot of how the

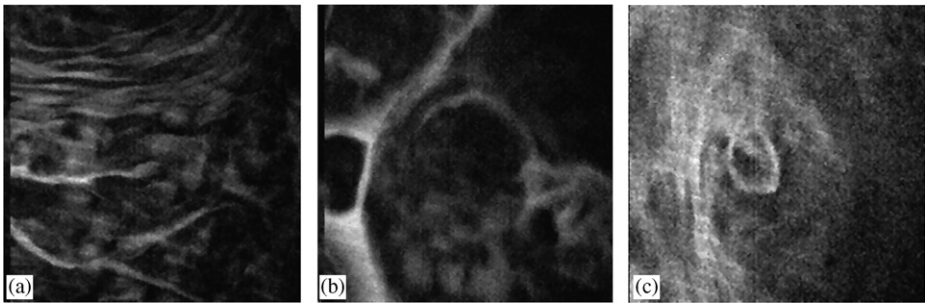

Fig. 5. Single frame images from real-time sequences of fluorescent images of the oral cavity stained with sodium fluorescein. Image width ~1.5 mm (a) tongue surface near the middle of the mouth, (b) tongue surface near the posterior of the mouth and (c) salivary duct at the posterior of the mouth.

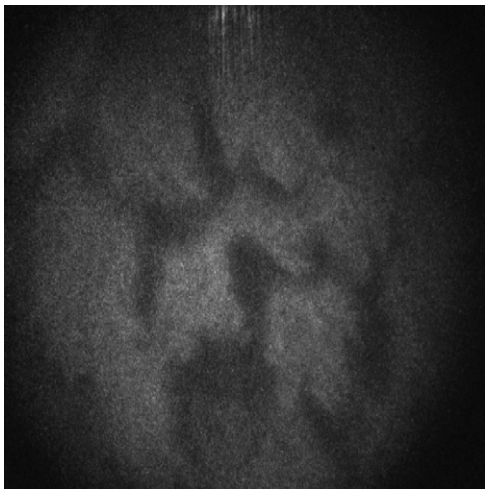

Fig. 6. Single frame image from a real-time sequences of fluorescent images of the residue remaining on the surface of the tongue after processing of 1.46 wt% CMC in TSS solution labelled with riboflavin. Image width ~1.5 mm.

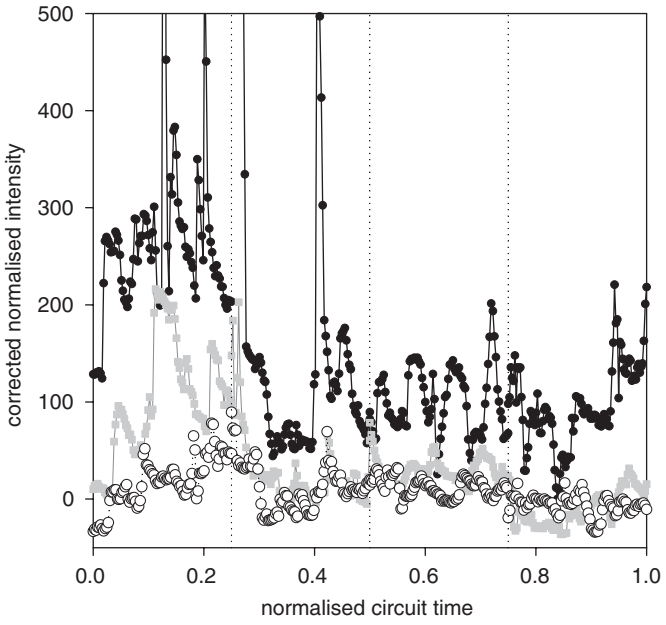

Fig. 7. Example intensity data for a sample of 1.46% CMC in TSS labelled with riboflavin. The y ordinate represents the average intensity over each frame corrected for the average intensity observed during a background scan recorded prior to any sample ingestion. This background subtraction ensures that the average signal is zero in the absence of any residue but does give rise to some negative values. The x ordinate represents the normalised path taken around the mouth. The different regions are marked by the vertical dotted lines with the region 0–0.25 relating to travelling from the tip to the back of the tongue along the right-hand edge of the tongue, 0.25–0.5 to crossing the back of the tongue, 0.5–0.75 to traversing the left-hand side of the tongue and 0.75–1 to the tip of the tongue. Traces are related to data collected at different times after the sample has been processed, —●— $t = 0$, immediately after expectoration; —■— $t = 5$ min; —○— $t = 10$ min.

overall intensity immediately after sample swilling and expectoration varies as a function of sample viscosity. There is a clear upward trend in the data indicating that as the viscosity of the sample increases more residue is left behind on the surface of the tongue. Previous studies have also found that oral residue is increased for more viscous materials (Goulet & Brudevold, 1986).

3.2.2. Influence of tastant level in homogeneous aqueous fluids

Citric acid was included in CMC solutions as a tastant known to influence salivary flow rate (Watanabe & Dawes, 1988). Indeed the addition of citric acid has a strong influence on this factor. Fig. 9 shows the increase in relative salivary flow rate (= stimulated flow rate/resting flow rate) as a function of acid content. It might be expected that an increase in salivary flow rate would reduce the amount of material that would remain in the mouth after processing. Fig. 10 shows a plot of the overall intensity immediately after expectoration of the sample for the series of acid containing solutions. Each of these solutions had the same viscosity. As can be seen from this plot there is no clear trend in the data indicating that acid content and hence salivary flow rate has no clear impact on the initial deposited amount.

Comparing data collected at different times after sample ingestion gives an idea of how quickly the mouth processes this residue and clears it from the oral cavity. Much of the previous work on oral clearance has been in the areas of dental or pharma and is related to dental health (see for example Bibby, Mundorff, Zero, & Almekinder, 1986) or the

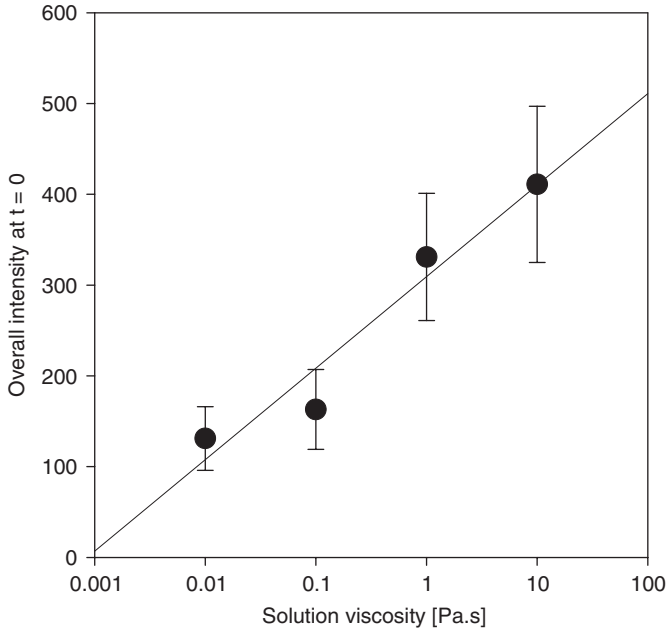

Fig. 8. Plot showing the overall intensities, related to amounts of CMC solution residue remaining on the tongue after oral processing, against viscosity of the solution. The error bars are calculated from the standard deviation in the mean intensity data. The line is a linear fit to the log data as a guide to the eye.

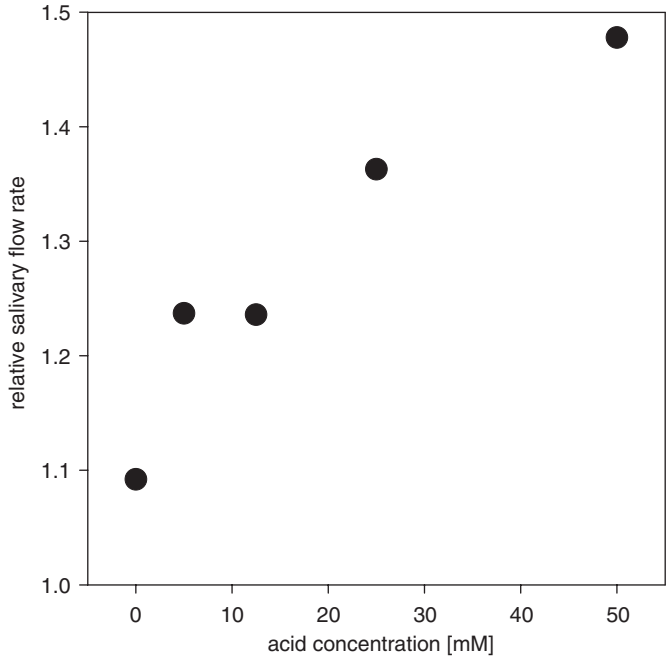

Fig. 9. Relative salivary flow rate (= stimulated flow rate/resting flow rate) as a function of citric acid concentration.

clearance of drugs (Weatherell, Robinson, & Rathbone, 1994) from the oral cavity rather than to the sensory perception and after-feel of foods. Studies involve removing samples from different sites around the mouth (see for example Bashir, Gustavsson, & Lagerlöf, 1995; Hanaki et al., 1993; Linke & Birkenfeld, 1999) or swill and/or spit studies (see for example Bashir, Ekberg, & Lagerlöf, 1995; Mor & McDougall, 1977; Vivien-Castioni, Gurny, Baehni, & Kaltsatos, 2000) followed by analysis of e.g. sugar, acid or fluoride. Here, we are concerned with residue of the actual product and the impact it may have on the perception of food after the main bolus has been swallowed (or expectorated). Again, higher salivary flow rates would be expected to exert a strong influence on this process. Fig. 11 shows an example plot of overall intensity as a function of time. Previous work looking at the clearance of citric acid from the oral cavity reported a bi-phasic clearance (Bashir, Ekberg et al., 1995; Bashir, Gustavsson et al., 1995). The data from the current study, which uses viscosified citric acid solutions, show no evidence of a two stage process, instead a single exponential fit (Eq. (1)) can be used to give a characteristic time, τ, for clearance of the residue.

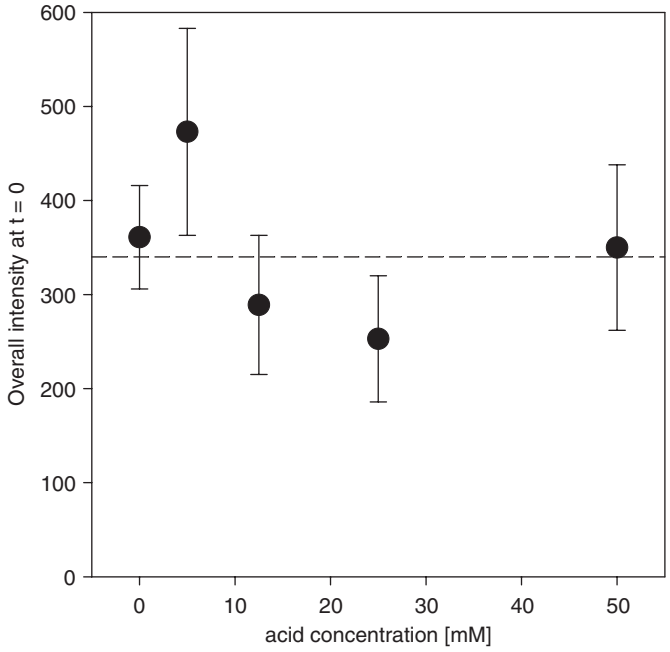

Fig. 10. Plot showing the overall intensities, related to amounts of CMC solution residue remaining on the tongue after oral processing, against concentration of citric acid. The error bars are calculated from the standard deviation in the mean intensity data. The flat line represents the average of the data and is a guide to the eye.

$$I = I_0 e^{-t/\tau}. \quad (1)$$

The oral clearance in the current study appears to be markedly faster than that reported by Bashir, Ekberg et al. (1995) and Bashir, Gustavsson et al. (1995). This may be due to the differences in viscosity between the two samples.

Dawes (1983) and Dawes and Watanabe (1987) have described a mathematical model of the role of saliva in oral clearance, with faster clearance expected for higher salivary flow rates. Fig. 12 clearly demonstrates this effect, with higher salivary flow rates leading to lower characteristic times and faster clearance.

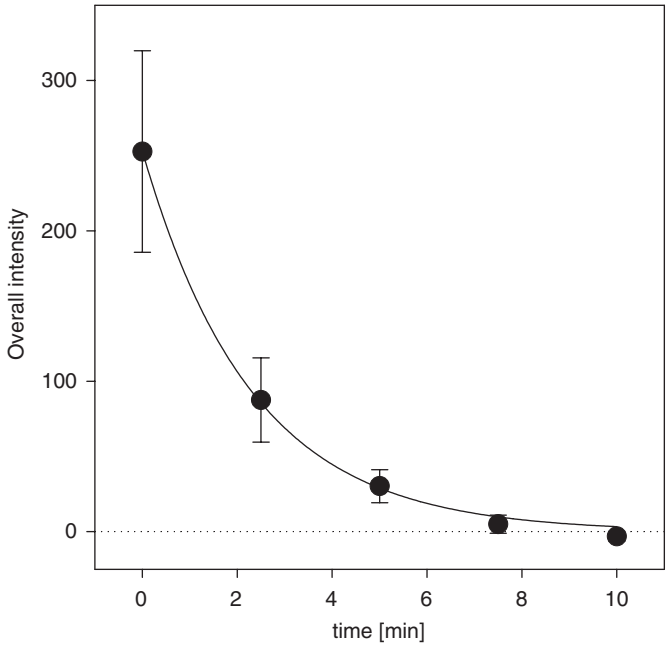

Fig. 11. Example clearance data for a sample of 1.46 wt% CMC in riboflavin-labelled TSS with 25 mM citric acid content. The solid symbols, ●, represent the overall average data and the solid line represents a single exponential fit to the data. The error bars are calculated from the standard deviation in the mean intensity data.

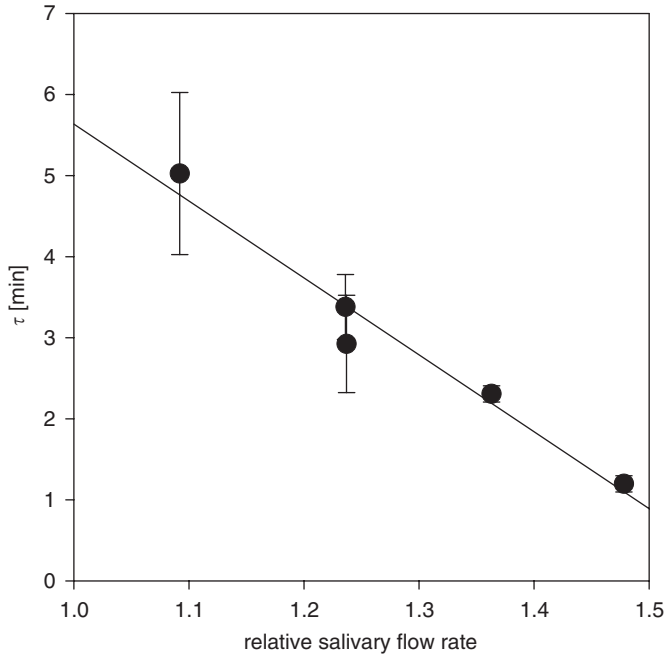

Fig. 12. Comparison of the characteristic time for clearance, τ, of a range of same viscosity CMC solutions as a function of relative salivary flow rate. Lower τ corresponds to faster clearance. The solid line is a linear fit to the data.

3.2.3. *Influence of viscosity in oil samples*

Example fluorescence images collected from the surface of the tongue after processing different viscosity oils are shown in Fig. 13. The oils were presented to the subject as homogeneous bulk samples. The images show very clear evidence of the emulsification that occurs during mouth processing of these fluids. Although Fig. 13a and b appear very similar, closer analysis of the droplet sizes in the images does show differences between the two samples. The higher viscosity castor oil gave an average droplet size of ~1.3 times that of the lower viscosity corn oil. Also, near the tip of the tongue, the emulsification process appears incomplete for castor oil and very large (many hundreds of micron) pools of oil are observed, Fig. 13c). No such pools were observed with the lower viscosity corn oil. If we assume that other parameters are approximately equal (shear history, interfacial energy and so on), this would indicate that droplet break up is a function of viscosity. The influence of viscosity on oil droplet break-up has been examined previously from an engineering perspective (Davies, 1987). Although under very different mixing conditions, the work of Davies (1987) also concluded that the droplet size would increase for more viscous oils. Because of the very different quantum yields and concentrations of dye used to label the two oils, a quantitative comparison of the residue amounts is not currently possible.

4. Conclusions

This work presents a novel combination of a rod lens-type rigid endoscope (suitable for clinical use) with a flexible light path allowing full axis of movement and video-rate imaging. High contrast all digital images that are capable of showing cellular level detail can be obtained comfortably from inside the oral cavity of a subject in natural pose. Useful imaging modes include endoscopic fluorescence and incoherent backscattered imaging. These modes are practical for both hard and soft tissues in the mouth and all in a single instrument. Using combinations of imaging modes cellular structures and vascular architecture can be examined and in particular, fluorescence imaging has been used to examine food material distributions and clearance behaviour.

The initial potential of this technique has been demonstrated through the study of a range of homogenous fluid foods in a single subject. The results indicate that for a range of different concentration CMC solutions, sample viscosity is a key indicator for amount of residue remaining in the oral cavity after oral processing. A second series of aqueous solutions with constant CMC concentration but varying citric acid concentration were examined to probe the effect of salivary flow rate. It was found, perhaps surprisingly, that salivary flow rate had little or no effect on the initially deposited amounts of residue. However, salivary flow rate was found to correlate strongly with the rate at which the residue was subsequently cleared from the tongue. Faster salivary flow rates (higher acid contents) induced faster clearance, indeed for an increase in relative salivary rate of a factor of 1.5, the sample was found to clear ~4 times faster. The technique has also been

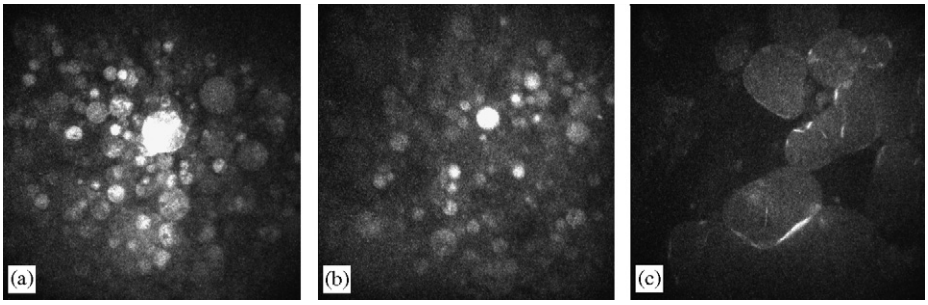

Fig. 13. Single frames from the video image recorded from the surface of the tongue immediately after 30 s oral processing of a bulk oil sample. (a) castor oil at the back right of the tongue, (b) corn at the back right of the tongue and (c) castor oil at the tip of the tongue. Image width is ~1.5 mm.

demonstrated to be useful for examining product structure breakdown by following the in-mouth emulsification of bulk oils.

This instrument opens up new possibilities for research into the range of processes that occur in the mouth during food processing. The technique could be employed to examine a wide variety of food materials ranging from the homogeneous fluids of the current study to particulates or solid foods and including multi-component foods. Indeed, dual channel imaging and careful selection of fluorescent labels will enable simultaneous investigation of two components of a multi-component food, for example the fat and aqueous phases of typical food emulsions. The technique also offers the potential to probe, not only residue amount, but also the spatial distribution of the residue as well as the length scales of any structure in the residue. The residue remaining from the processing of real foods, providing that they can be adequately labelled, could also be easily imaged. Ultimately, it is the material that is in contact with the tongue surface that is responsible for much of the sensory impact of a product and enabling a direct measure of the undisrupted residue should provide a wealth of information and could play a pivotal role in increasing our understanding of food material behaviour in use and its impact on sensory perception of food materials.

Acknowledgements

The authors would like to acknowledge the help of Ingrid Appelqvist, Unilever Research Vlaardingen, in this work.

References

Bashir, E., Ekberg, O., & Lagerlöf, F. (1995). Salivary clearance of citric acid after an oral rinse. *Journal of Dentistry*, *23*, 209–212.

Bashir, E., Gustavsson, A., & Lagerlöf, F. (1995). Site-specificity of citric-acid retention after an oral rinse. *Caries Research*, *29*, 467–469.

Bibby, B. G., Mundorff, S. A., Zero, D. T., & Almekinder, K. J. (1986). Oral food clearance and the pH of plaque and saliva. *Journal of the American Dental Association*, *112*, 333–337.

Bourne, M. C. (2002). *Food texture and viscosity—concept and measurement*. London: Academic Press.

British Standard Safety of Laser Products BS EN 60825-1:1994.

Davies, J. T. (1987). A physical interpretation of drop sizes in homogenizers and agitated tanks, including the dispersion of viscous oils. *Chemical Engineering Science*, *42*, 1671–1676.

Dawes, C. (1983). A mathematical-model of salivary clearance of sugar from the oral cavity. *Caries Research*, *17*, 321–334.

Dawes, C., & Watanabe, S. (1987). The effect of taste adaptation on salivary flow-rate and salivary sugar clearance. *Journal of Dental Research*, *66*, 740–744.

De Wijk, R. A., Engelen, L., & Prinz, J. F. (2003). The role of intra-oral manipulation in the perception of sensory attributes. *Appetite*, *40*, 1–7.

Engelen, L., de Wijk, R. A., Prinz, J. F., Janssen, A. M., van der Bilt, A., Weenen, H., et al. (2003). A comparison of the effects of added saliva, alpha-amylase and water on texture perception in semisolids. *Physiology and Behavior*, *78*, 805–811.

Engelen, L., de Wijk, R. A., Prinz, J. F., van der Bilt, A., & Bosman, F. (2003). The relation between saliva flow after different stimulations and the perception of flavor and texture attributes in custard desserts. *Physiology and Behavior*, *78*, 165–169.

Goulet, D., & Brudevold, F. (1986). The effects of viscosity on oral clearance of glucose. *Journal of Dental Research*, *65*, 283.

Hanaki, M., Nakagaki, H., Nakamura, H., Kondo, K., Weatherell, J. A., & Robinson, C. (1993). Glucose clearance from different surfaces of human central incisors and 1st molars. *Archives of Oral Biology*, *38*, 479–482.

Kringelback, M. L., O'Doherty, J., Rolls, E. T., & Andrews, C. (2003). Activation of the human orbitofrontal cortex to a liquid food stimulus is correlated with its subjective pleasantness. *Cerebral Cortex*, *13*, 1064–1071.

Linke, H. A. B., & Birkenfeld, L. H. (1999). Clearance and metabolism of starch foods in the oral cavity. *Annals of Nutrition and Metabolism*, *43*, 131–139.

Lucas, P. W., Prinz, J. F., Agrawal, K. R., & Bruce, I. C. (2002). Food physics and oral physilogy. *Food Quality and Preference*, *13*, 203–213.

Moskowitz, H. R. (Ed.). (1987). *Food texture instrumental and sensory measurement*. New York: Marcel Dekker.

Mor, B. M., & McDougall, W. A. (1977). Effects of milk on ph of plaque and salivary sediment and the oral clearance of milk. *Caries Research*, *11*, 223–230.

Peleg, M. (2006). On fundamental issues in texture evaluation adn texturization—a view. *Food Hydrocolloids*, *20*, 405–414.

Vingerhoeds, M. H., Blijdenstein, T. B. J., Zoet, F. D., & van Aken, G. A. (2005). Emulsion flocculation induced by saliva and mucin. *Food Hydrocolloids*, *19*, 915–922.

Vivien-Castioni, N., Gurny, R., Baehni, P., & Kaltsatos, V. (2000). Salivary fluoride concentrations following applications of bioadhesive tablets and mouthrinses. *European Journal of Pharmaceutics and Biopharmaceutics*, *49*, 27–33.

Watanabe, S., & Dawes, C. (1988). The effects of different foods and concentrations of citric acid on the flow rate of whole saliva in man. *Archives of Oral Biology*, *33*, 1–5.

Watson, T. F., Neil, M. A. A., Juskaitis, R., Cook, R. J., & Wilson, T. (2002). Video-rate confocal endoscopy. *Journal of Microscopy*, *207*, 37–42.

Weatherell, J. A., Robinson, C., & Rathbone, M. J. (1994). Site-specific differences in the salivary concentrations of substances in the oral cavity—implications for the etiology of oral-disease and local-drug delivery. *Advanced Drug Delivery Reviews*, *13*, 23–42.